The role of the Bronsted and Lewis acidic site balance of Sulfonated, Zr-MCM-41 catalysts in cellulose conversion towards 5-hydroxymethyl furfural

Son Tung Pham[1,2], Ba Manh Nguyen[1], Giang H Le[1], Andras Sapi[3,4,*], Imre Szenti[3,5], Zoltan Konya[3,5] and Tuan A Vu[1]

[1]*Institute of Chemistry, Vietnam Academy of Science and Technology (VAST), Hanoi, Vietnam*

[2]*Vietnam National University (VNU), Hanoi, Vietnam*

[3]*University of Szeged, Interdisciplinary Excellence Centre, Department of Applied and Environmental Chemistry, H-6720, Rerrich Béla tér 1, Szeged, Hungary*

[4]*University of Szeged, Institute of Environmental and Engineering Sciences, H-6720 Szeged, Rerrich béla tér 1, Szeged, Hungary*

[5]*MTA-SZTE Reaction Kinetics and Surface Chemistry Research Group, University of Szeged, H-6720 Szeged, Rerrich Béla tér 1, Szeged, Hungary*

*Corresponding author: sapia@chem.u-szeged.hu

ABSTRACT

Sulfonated and Zr-loaded MCM-41 structures with different Zr-loading were successfully synthesized by direct incorporation of Zr into MCM-41 framework followed by sulfonation. The samples were characterized by XRD, FTIR, HR-TEM, BET, EDX and NH_3-TPD. From XRD and BET results, the meso-structure of MCM-41 material with high surface area was revealed. HR-TEM images showed the formation of cluster-free mesopore skeleton framework. NH_3-TPD result confirmed the presence of Bronsted acidic and lewis acidic sites in S-Zr-MCM-41 catalysts. S-Zr-MCM-41 with 15 % of Zr-loading exhibited the highest cellulose conversion (65-70%) and 5-Hydroxymethyl furfural selectivity (16 %), which is attributed to the high ratio of the Bronsted-to-Lewis acidic sites.

Keywords: Sulfonated Zr-MCM-41 materials, Zr incorporation into MCM-41 framework, Cellulose conversion to 5-HMF

1. Introduction

5-hydroxymethyl furfural (5-HMF) has been reported as a major platform chemical that could be produced from hemicellulose and cellulose by hydrolysis in acid medium [1-3]. HMF is a versatile intermediate between biomass-based carbohydrate chemistry and petroleum-based industrial chemistry with potential use in production of chemicals and fuels [4,5]. Production of HMF from cellulose requires 3 step catalytic mechanism involving: hydrolysis of cellulose to glucose catalyzed by a Brønsted acid, isomerization of glucose to fructose by lewis acid assistance and dehydration of fructose to 5-HMF by a Brønsted acid [6]. To convert cellulose into HMF, several homogeneous catalysts have been used including H_2SO_4, HCl-$AlCl_3$, $CrCl_2$-$CrCl_3$, $ZrOCl_2$/$CrCl_3$ [7-11]. However, the use of homogeneous catalysts is limited, regarding environmental issues and drawbacks with respect to the corrosion, toxicity, difficulty of catalyst separation-recovery, creation of huge solid waste [12]. To overcome these limitations, recently, the usage of solid acid catalysts in the conversion of cellulose to HMF has received a great interest [13-17].

As mentioned above, conversion of cellulose to HMF is catalyzed by both Brønsted and lewis acid sites. For this purpose, bifunctional solid acid catalysts have been developed and used [18-21]. Mazzotta et al [21] reported the high effectiveness of Ti(IV)-HSO_3 catalyst for dehydration of cellulose, glucose and fructose. They depicted the possible dual role of the Brønsted and lewis acid sites for the facile bio-mass conversion.

Osatiashtiani et al [18] have used bifunctional sulfonated zirconia catalyst for conversion of glucose to HMF and showed high effectiveness of this catalyst. Additionally, higher effectiveness was obtained when they used the sulfonated zirconia impregnated on mesoporous silica SBA-15 [19]. Mesoporous silica like SBA-15, MCM-41 has widely been used as effective supports due to the high surface area (600-1000 m^2/g) and large pore size (5-10 nm) [22-24].

In the present work, we report the synthesis of S-Zr-MCM-41 catalysts by direct incorporation of Zr into MCM-41 framework followed by sulfonation. Catalytic activity and selectivity of S-Zr-MCM-41 samples in the conversion of cellulose to 5-hydroxymethyl furfural were tested and evaluated. The role of Brønsted and lewis acid sites on the catalytic performance was also discussed.

2. Experimental

2.1. Synthesis of S-Zr-MCM-41 materials

Chemicals: $ZrSO_4$ (Aldrich), TEOS (Aldrich), NH_4OH solution (25%), CTABr ((Aldrich), 1-butyl-3imidazium cloride (Aldrich), H_2SO_4 (98% concentration).

Zr-MCM-41 samples were synthesized by hydrothermal treatment, according to the procedure described by Chen et al [25]. Zr-MCM-41 mesoporous materials were prepared with Zr/Si ratio of 4 - 20% (in weight) using $ZrSO_4$ and TEOS as Zr and Si source, respectively where CTABr used as a template. The certain amounts of $ZrSO_4$, TEOS, CTABr and NH_4OH solution were introduced into a beaker and stirred in a glass bath until homogeneous gel was obtained. The gel was poured into a teflon-lined autoclave for crystallizing in a furnace at 100 ^oC for 24h. Products were separated by centrifuge apparatus and then they were washed, dried and calcined at 550 ^oC for 4h. The obtained samples were sulfonated by treatment with sulfuric acid solution of 1.0 M at room temperature for 1 h. Sulfonated Zr-MCM41 samples were washed with the destillated water and then dried in a furnace at 100 ^oC, overnight.

The obtained samples are denoted as S-4Zr-MCM-41; S-8Zr-MCM-41; S-12Zr-MCM-41; S-15Zr-MCM-41 and S-20Zr-MCM-41 with respect to 4, 8, 12, 15 and 20% Zr loading.

2.2. Characterization of S-Zr-MCM-41

MCM-41 and S-Zr-MCM-41 samples are characterized by XRD performed on D8 Advance (Germany). TEM images were collected on a FEI TECNAI G2 20 X-Twin high-resolution transmission electron microscope (equipped with electron diffraction) operating at an accelerating voltage of 200 kV, where the samples were drop-cast onto carbon film coated copper grids from ethanol suspension. Energy Dispersive spectroscopic investigation was registered on an S-4700 scanning electron microscope (SEM, Hitachi, Japan) with accelerating voltage of 10-18 kV. FTIR was performed on JASCO (USA) machine FT-IR-4100. TPD-NH_3 measurements were performed on Autochem II with a heating speed of 10^oC/min.

2.3. Cellulose conversion reaction into 5-HMF

The conversion of cellulose to 5-HMF using S-Zr-MCM-41 catalysts was carried out in a teflon-lined stainless steel device equipped with a stirring system. A mixture of 2g cellulose, 0.2 g of catalyst, and 10 ml of water were poured into a reactor. Under the reaction conditions of reaction temperature of 170^{o}C, reaction time of 2h, heating speed of 10^{o}C/min and stirring speed of 250 rotations/min. Reaction products were obtained from separation of solid catalyst by using centrifuge apparatus. The product was analyzed by GC/MS Instruments - Agilent.

3. Results and Discussion

3.1. X-Ray Difraction (XRD)

XRD patterns of sulfonated Zr-MCM-41 sample are shown in Figure 1. As observed in figure 1a, all S-Zr-MCM-41 samples showed an intense peak at 2θ of 2^{o}, 3.7^{o} and 4.4^{o} attributed to the reflecting plane of (100), (110) and (200), respectively. These reféections are characteristic for the hexagonally ordered structure of MCM-41. However, in XRD patterns at large angle (Figure 1b), the typical peaks of ZrO_2 structure did not appeared. This may be explained by the fact that the Zr is doped into the structure or ionic exchange postion of the MCM-41 or the size and amount of the incorporated ZrO_2 clusters was too small, so it can not be detected by XRD.

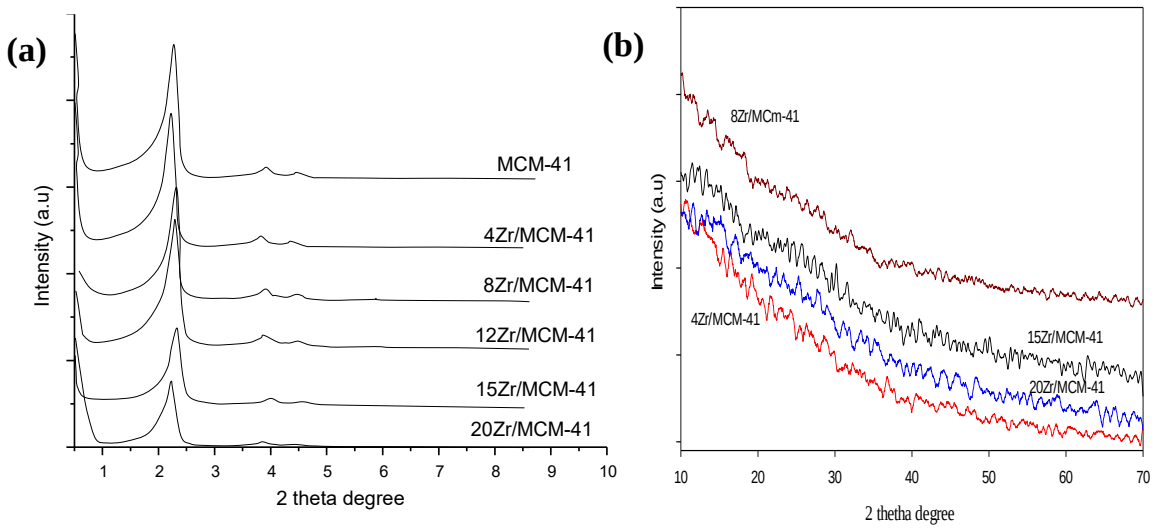

Figure 1. XRD patterns of S-Zr-MCM-41 samples at small angle (a) and large angle (b)

Table 1. presents the lattice parameters (d_{100} and a_o) of S-Zr-MCM-41 with different Zr loading. The distance and lattice constant increased with increasing Zr substitution degree. Note that Zr^{4+} ion larger than Si^{4+} ion, so Si substitution by Zr causes the increase of latice parameters. However, at high Zr loading (20% Zr) lattice parameters did not increase but they decrease. This indicated that a part of Zr was existed as an extra framework Zr.

Table 1. Latice paramenters (d_{100} and a_o) of S-Zr-MCM-41 samples

Sample	d_{100}(A^o)	a_o(nm)
MCM-41	39.2	45.3
S-4Zr/MCM-41	39.3	45.3
S-8Zr/MCM-41	39.4	45.5
S-12Zr/MCM-41	42.7	49.4
S-15Zr/MCM-41	43.4	50.1
S-20Zr/MCM-41	42.3	48.9

3.2. Fourier Transform Infrared spectroscopy (FTIR)

As observed in figure 2, in the FTIR spectra of all S-Zr-MCM-41 samples, the peak of Si-OH group at 3450 cm^{-1} appeared. The peak at 1640 cm^{-1} assigned to the H-O-H deformation vibration, the peak at 1084 cm^{-1}, characteristic for O–S-O symmetric valence vibration, the peak at 825 cm^{-1} and 550 cm^{-1} attributed to Si-O and Zr-O group, respectively [26-28].

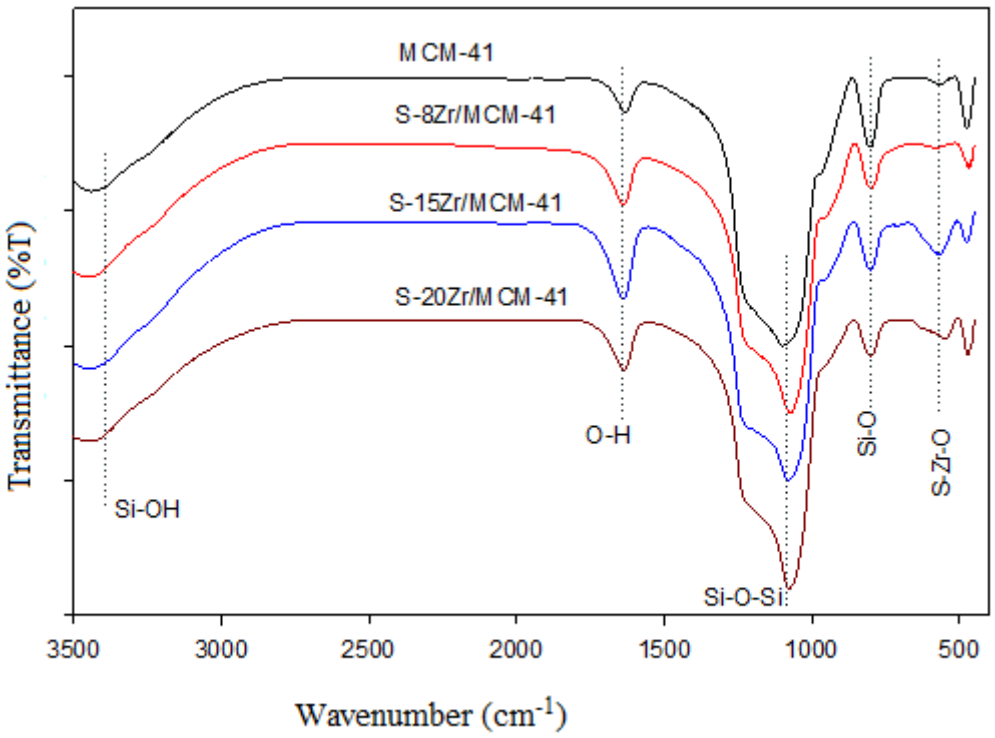

Figure 2. FTIR spectra of S-Zr-MCM-41 samples

3.3. Transmission Electron Microscopy (TEM)

The ordered pore structure of MCM-41 based samples is obvious at the TEM images (Figure 3). HR-TEM images of the MCM-41 catalysts with different Zr-loading (8-20 wt%) shows the absence of particles or nanoparticles corresponding to the Zr-based oxide structures. These phenomena correlate with the XRD results (Figure 1.) and show that the Zr is incorporated into the mesopore structure of the MCM-41.

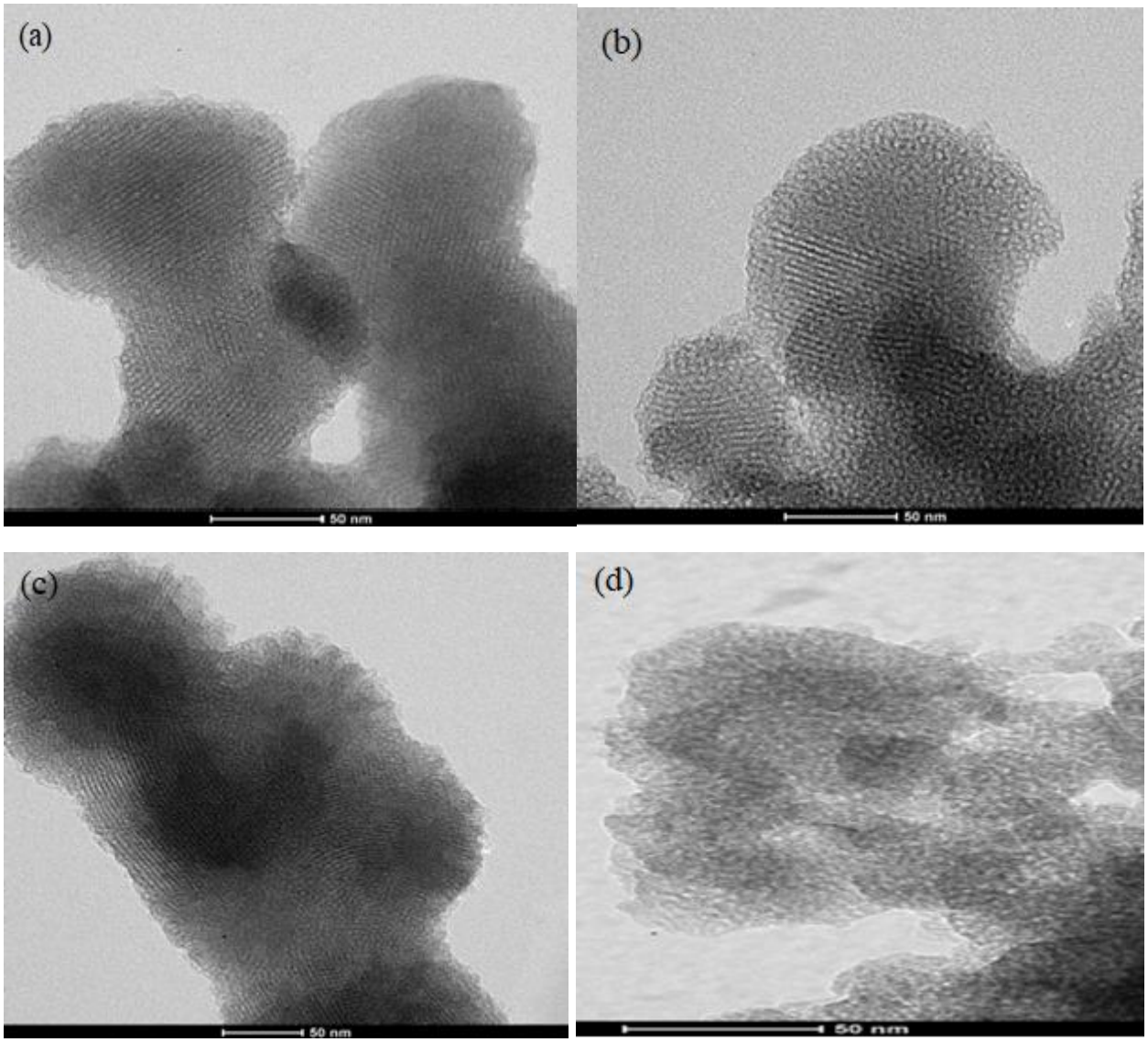

Figure 3. HR-TEM images of MCM-41 (a) S-8Zr-MCM-41 (b) S-15Zr-MCM-41 (c) and S-20Zr-MCM-41 sample (d)

3.3. Energy Dispersive X-Ray spectroscopy (EDX)

Zr content in solid S-Zr-MCM-41 samples was determined by EDX. Table 2. shows the elemental composition of S-Zr-MCM-41 catalysts. The Zr content in solid product increased with increasing Zr content in the gels and the amount of Zr in solid product is closed to that of the pristine gel. It is interesting to note that the Zr content was 16.8 % in the case of S-20Zr-MCM-41 sample showing that the structural skeleton is not able to uptake the initial 20% of the Zr. The success of the sulphurization was indicated by the presence of ~10 wt% of sulphur in the samples regardless of the Zr content.

Table 2. Element composition (wt%) of S-Zr-MCM-41 samples

Sample	Silicon (% wt)	Zirconium (% wt)	Sulfur (% wt)	Total
S-4Zr-MCM-41	85.95	3.84	10.21	100
S-8Zr-MCM-41	81.27	7.23	11.50	100
S-12Zr-MCM-41	77.73	10.02	12.25	100
S-15Zr-MCM-41	73.44	14.78	11.78	100
S-20Zr-MCM-41	69.54	16.78	10.68	100

3.4. N_2 adsorption –desorption, isotherms (BET)

From the adsorption-desorption isotherm of the sample MCM-41 (Figure 4.), the formation of the hysteresis loop at P/Po of 0.85 was observed. This is a typical feature of the mesoporous materials. Thus, for microporous materials, no hysteresis loop appeared. This hysteresis is due to the pores of large size (meso pore) causing the capillary condensation of nitrogen. All S-Zr-MCM-41 samples showed high surface area of 870 -1200 m^2/g and mesopore volume of 0.74-1.27 cm^3/g (Table 3.). However, with increasing the Zr content, mesopore volume and pore diameter decreased. This indicated the deformation effect of Zr-ions incorporated into the structure of the MCM-41 skeleton. Thus, with increasing Zr-loading, the meso-pore volume and pore diameter decreased at the extent of 50-60%.

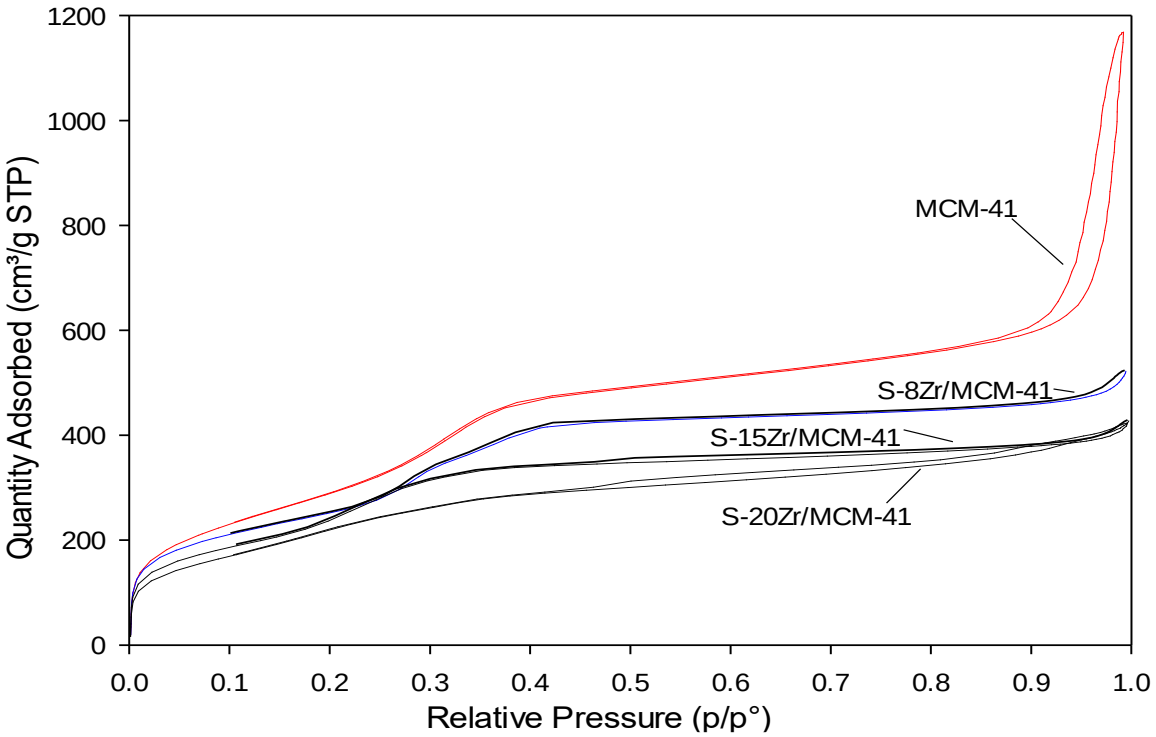

Figure 4. N_2 adsorption –desorption isotherms of MCM-41 and S-Zr-MCM-41 samples

Table 3. Textual characteristics of MCM-41 and S-Zr-MCM-41 samples

Sample	S_{BET} (m^2/g)	$S_{mesopore}$ (m^2/g)	V_{pore} (cm^3/g)	D (nm)
MCM-41	1190.7	826.2	1.99	6.0-6.1
S-4Zr-MCM-41	1242.6	824.5	1.27	3.6-3.7
S-8Zr-MCM-41	1040.1	663.6	0.91	3.4-3.5
S-12Zr-MCM-41	912.8	600.8	0.85	3.5-3.6
S-15Zr-MCM-41	1021.6	590.9	0.75	3.0-3.1
S-20Zr-MCM-41	873.9	574.5	0.74	3.3-3.6

3.5. Temperature programed desorption of NH_3 (NH_3-TPD)

NH_3-TPD profiles of S-Zr-MCM-41 with different Zr loading are showed in Figure 5. For all S-Zr-MCM-41 samples, NH_3 desorbed at T_{max} of 140-170 ^oC, 250-270 ^oC and 470-570 ^oC which correspond to the weak (physisorbed NH_3), Bronsted acidic and Lewis acidic sites, respectively [29]. As literature mentioned before [18-21], it is posibble that in the case of the S-Zr-MCM-41 samples, both Bronsted and lewis acid sites are formed. Thus, the substitution of Si^{4+} by Zr^{4+} leads to create the lewis acid sites and the sulfonation of Zr-MCM-41 leads to create the Bronsted acid sites H-SO_3^-.

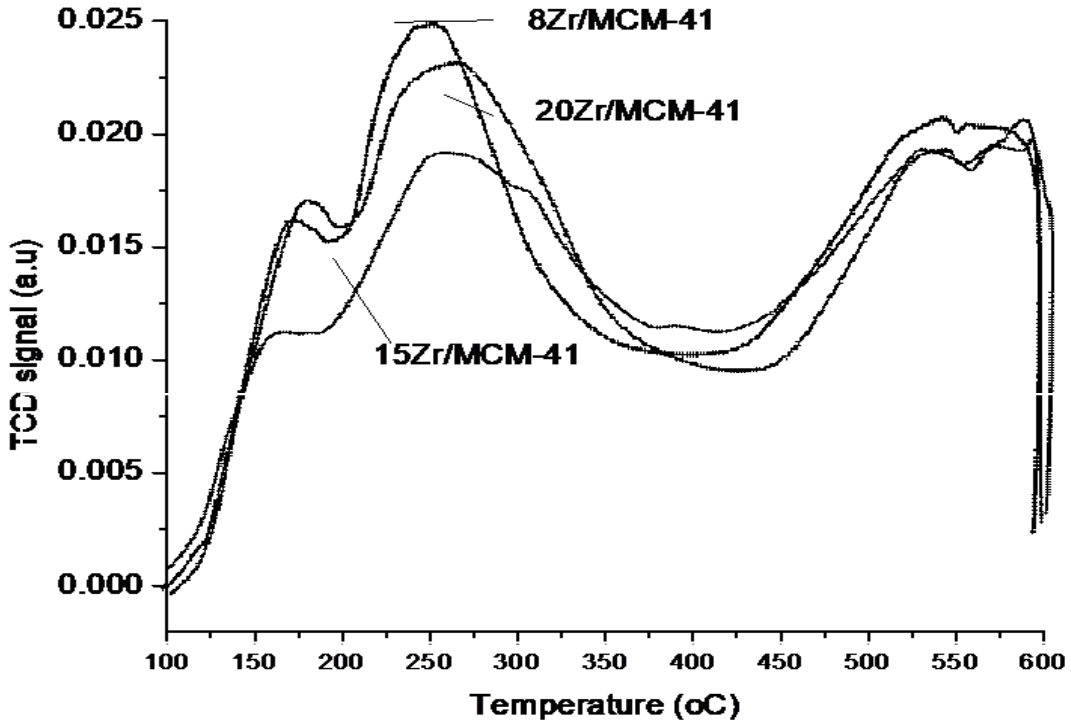

Figure 5. NH_3-TPD profiles of S-Zr-MCM-41 with different Zr loading content

The amount of NH_3 desorbed for S-Zr-MCM-41 sample is different, depending on the Zr loading (Table 4). For the S-Zr-MCM-41 with 8 wt% Zr loading has the most amount of surface lewis acidic sites. In the case of the Broensted acidic sites, the amount of the sites were following the S-15Zr/MCM-41, S-8Zr/MCM-41 and S-20Zr/MCM-41 pattern. It is clearly seen, that the ratio of the Broensted acidic sites and the Lewis acidic sites is different and depends on the Zr loading. Thus, the substitution

of Si^{4+} by Zr^{4+} leads to create the lewis acid sites and the sulfonation of Zr-MCM-41 leads to create the Brønsted acid sites of $–H\text{-}SO_3^-$. However, the amount of the sites are not correlate with the amount of Zr or/and S loading of the catalysts. The synergetics of the skeleton structure, Zr-loading and surface sulphur concetration leads to the special amounts and ratios of the different acidic sites.

Table 4. NH_3 amount desorbed at different temperature for S-Zr-MCM-41 with different Zr loading

Sample	mmol desorbed NH_3/g S-Zr-MCM-41 at different temperature range			Total mmol NH_3
	T_{max} 140 -170 ^oC	T_{max} 250-270 ^oC	T_{max} 470 -570 ^oC	T_{max} 140-570 ^oC
S-8Zr/MCM-41	0.415	0.799	0.593	1.807
S-15Zr/MCM-41	0.404	0.986	0.419	1.809
S-20Zr/MCM-41	0.385	0.49	0.384	1.259

3.6. Conversion of cellulose to 5-HMF

From the proposed mechanism in the literature, conversion of cellulose to 5-HMF occurs through three step reaction: Hydrolysis of cellulose to glucose catalyzed by Brønsted acid sites, isomerization of glucose to fructose mediated by lewis acid sites and dehydration of fructose to 5-HMF facilitated by Brønsted acid sites. Therefore, cellulose conversion to 5-HMF needs both Brønsted and lewis acid sites. S-Zr-MCM-41 catalysts contain both Brønsted and lewis acid sites corresponding to the NH_3-TPD results.

Catalytic performance (activity and selectivity) of sulfonated Zr-MCM-41 catalysts in the cellulose conversion to 5-HMF was presented in the table 5. All S-Zr-MCM-41 samples regardless to the Zr-loading exhibited high conversion of 63 -70%. However, selectivity torward to 5-HMF between S-Zr-MCM-41 samples was

considerably differentiated. The selectivity was increasing with the Zr-loading upto 15%. The highest activity and selectivity was produced by the S-15Zr-MCM-41 catalyst. This sample has one of the highest surface area, while the pore volume and surface area distribution of mesopores were decent compared to the other catalysts. It is interesting to note, that this catalyst has the most Bronsted acidic sites and the ration of the Bronsted acid and the Lewis acidic sites are the highest, too (~2.5) compared to other MCM-41-based samples. The balance of Lewis and Bronsted acid sites and the improvement of 5-HMF selectivity by using the catalysts with the high Lewis/bronsted acid sites ratio were reported [30, 31]. In the future, S-Zr-MCM-41 sample will be treated with milder sulfonation condition by using the diluated H_2SO_4 concentration towards higher 5-HMF selectivity.

Table 5. Catalytic performance of S-Zr-MCM-41 catalysts in the conversion of cellulose to 5-HMF

Sample	**C(%)**	**S (%)**	**Y(%)**
S-4Zr-MCM-41	63.27	2.99	1.89
S-8Zr-MCM-41	64.51	10.60	6.83
S-12Zr-MCM-41	69.48	11.37	9.02
S-15Zr-MCM-41	*70.15*	*16.39*	*11.49*
S-20Zr-MCM-41	68.63	9.39	6.44

Conclusions

From the obtained results, some conclusions could be drawn:

• A serie of S-Zr-MCM-41 with different Zr loading was successfully synthesized by direct incorporation of Zr into MCM-41 framework and followed by sulfonation.

• S-Zr-MCM41 samples were characterized by XRD, FTIR, HR-TEM, BET, EDX and NH_3-TPD. From XRD and BET results, it revealed the meso-structure of MCM-41 material. HR-TEM images showed the formation of cluster-free MCM-41

structures. NH_3-TPD result confirmed the presence of Bronsted as well as Lewis acidic sites in S-Zr-MCM-41 catalysts, which catalyst has the most Bronsted acidic sites and the highest ratio of the Bronsted acid and the Lewis acidic sites.

Acknowledgments: The authors would like to thank the Institute of Chemistry - VAST for funding the project (QTHU 01.01/18-19). This paper was supported by the Hungarian Research Development and Innovation Office through grants NKFIH OTKA PD 120877 of AS and K120115 of KZ. The financial support of the Hungarian National Research, Development and Innovation Office through the GINOP-2.3.2-15-2016-00013 project "Intelligent materials based on functional surfaces - from syntheses to applications" and the Ministry of Human Capacities through the EFOP-3.6.1-16-2016-00014 and 20391-3/2018/FEKUSTRAT project is also acknowledged.

References

1. Lewkowski, J. Synthesis, chemistry and applications of 5-hydroxymethyl-furfural and its derivatives. Arkivoc 2001, 1, 17–54.

2. Van Putten R. J; van der Waal J. C; de Jong E; Rasrendra C. B; Heeres H. J; de Vries J. G. Hydroxymethylfurfural, a versatile platform chemical made from renewable resources. Chem. Rev. 2013, 113,1499–1597.

3. Bozell J. J; Petersen G. R. Technology development for the production of biobased products from biorefinery carbohydrates- The US department of energy's "top 10" revisited. Green Chem. 2010, 12, 539–554.

4. De Jong E; Dam M; Sipos L Gruter, G Furandicarboxylic acid (FDCA), a versatile building block for a very interesting class of polyesters. Biobased Monomers Polym. Mater. 2012, 1105, 1–13.

5. Zhong, S.; Daniel, R.; Xu, H.; Zhang, J.; Turner, D.; Wyszynski, M.L.; Richards, P. Combustion and emissions of 2,5-dimethylfuran in a direct-injection spark-ignition engine. Energy Fuels 2010, 24, 2891–2899.

6. Osatiashtiani, A.; Lee, A.F.; Brown, D.R.; Melero, J. A. Morales, G.; Wilson, K. Bifunctional SO4/ZrO2 catalysts for 5-hydroxymethylfufural (5-HMF) production from glucose. Catal. Sci. Technol. 2014, 4, 333–342.

7. Yang Y, Hu C, Abu-Omar. Conversion of carbohydrates and lignocellulosic biomass into 5-hydroxymethylfurfural using $AlCl_3.6H_2O$ catalyst in a biphasic solventsystem. (2012) Green Chem 14: 509-513

8. Pagán-Torres YJ, Wang T, Gallo JMR, Shanks BH, Dumesic JA. Production of 5-hydroxymethylfurfural from glucose using a combination of lewis and brønsted acid catalysts in water in a biphasic reactor with an alkylphenol solvent *Acs Catalysis*. 2: 930-934

9. Zhao H, Holladay JE, Brown H, Zhang ZC. Metal chlorides in ionic liquid solvents convert sugars to 5-hydroxymethylfurfural. (2007) Science 316: 1597- 1600.

10. Chan JYG, Zhang Y. Selective Conversion of Fructose to 5-Hydroxymethyl furfural Catalyzed by Tungsten Salts at Low Temperatures. (2009) ChemSusChem 2: 731-734.

11. Hu S, Zhang Z, Song J, Zhou Y, Han B. Efficient conversion of glucose into 5-hydroxymethylfurfural catalyzed by a common Lewis acid $SnCl_4$ in an ionic liquid. (2009) Green Chem 11: 1746- 1749

12. Zhang S, Li W, Zeng X, Sun Y, Lin L. Catalytic conversion of biomass-derived carbohydrates into 5-hydroxymethylfurfural using a strong solid acid catalyst in aqueous γ-valerolactone. (2014) BioResources 9: 4656-4666.

13. Sanan Eminov, Paraskevi Filippousi, Agnieszka Brandt, James D. E. T. Wilton-Ely, and Jason P. Hallett. Direct Catalytic Conversion of Cellulose to 5-Hydroxymethylfurfural Using Ionic Liquids. Received: 21 June 2016; Accepted: 11 October 2016; Published: 20 October 2016.

14. Asim Bhaumik and Piyali Bhanja. Biomass to Bioenergy over Porous Nanomaterials: A Green Technology. *Trends in Green Chemistry* 1 (2015) 1-8.

15. Federica Menegazzo, Elena Ghedini, and Michela Signoretto. 5-Hydroxymethylfurfural (HMF) Production from Real Biomasses. Molecules. 2018 Sep; 23(9): 2201.

16. Karen Wilson and Adam F. Lee. Catalyst design for biorefining. Philosophical Transactions A. Published:28 February 2016. https://doi.org/10.1098/rsta.2015.0081

17. Hara M, Nakajima K, Kamata K. Recent progress in the development of solid catalysts for biomass conversion into high value-added chemicals. Sci Technol Adv Mater. 2015 May 20;16(3):034903. eCollection 2015 Jun.

18. Osatiashtiani A, Lee AF, Brown DR, Melero JA, Morales G. Bifunctional SO_4/ZrO_2 catalysts for 5-hydroxymethylfufural (5-HMF) production from glucose. (2014) Catal Sci Technol 4: 333–342.

19. Osatiashtiani A, Lee AF, Granollers M, Brown DR, Olivi L. Hydrothermally stable, conformal, sulfated zirconia monolayer catalysts for glucose conversion to 5-HMF. (2015) ACS Catal 5: 4345-4352.

20. Lai DM, Deng L, Guo QX, Fu Y. Hydrolysis of biomass by magnetic solid acid.

(2011) Energy Environ Sci 4: 3552-3557.

21. Mazzotta MG, Gupta D, Saha B, Patra AK, Bhaumik A. Nano-(Bio)Catalysis in Lignocellulosic Biomass Valorization. (2014) ChemSusChem 7: 2342-2350.

22. Novak MAS, Holewinski A, Hoyt CB, Yoo CJ, Chai SH. Probing the Role of Zr Addition versus Textural Properties in Enhancement of CO_2 Adsorption Performance in Silica/PEI Composite Sorbents. (2015) Langmuir 31: 9356-9365.

23. Ogino I, Suzuki Y, Muka SR. Tuning the Pore Structure and Surface Properties of Carbon-Based Acid Catalysts for Liquid-Phase Reactions. (2015) ACS Catal 5: 4951-4958.

24. Seelandt B, Wark M. Electrodeposited Prussian Blue in mesoporous TiO_2 as electrochromic hybrid material. (2012) Microporous Mesoporous Mater 164: 67-70.

25. L. F. Chen·, J.A.Wang, L. E. Noreña, J. Aguilar, J. Navarrete, P. Salas, J. A. Montoya, P. Del Ángel . Synt hesis and physicochemical properties of Zr-MCM-41 mesoporous molecular sieves and $Pt/H_3PW_{12}O_{40}$/Zr-MCM-41 catalysts. Journal of Solid State Chemistry Volume 180, Issue 10, October 2007, Pages 2958-2972.

26. M.S.A. Salam, M.A. Betiha, S.A. Shaban, A.M. Elsabagh, R.M.A. El-Aal, F.Y. El Kady Synthesis and characterization of MCM-41-supported nano zirconia catalysts, E*gypt. J. Pet.*, 24 (2015), pp. 49-57

27. A. Derylo-Marczewska, W. Gac, N. Popivnyak, G. Zukocinski, S. Pasieczna, The influence of preparation method on the structure and redox properties of mesoporous Mn-MCM-41 materials, *Catal. Today* 114 (2006) 293.

28. L. Wang, A. Kong, B. Chen, H. Ding, Y. Shan, M. He, Mol. Direct synthesis, characterization of Cu-SBA-15 and its high catalytic activity in hydroxylation of phenol by H_2O_2, *Catal. A Chem.* 230 (2005) 143.

29. András Sápi, Upendar Kashaboina, Kornélia B. Ábrahámné, Juan Fernando Goméz-Peréz, Imre Szenti, Gyula Halasi¸ János Kiss, Balázs Nagy, Tamás Varga, Ákos Kukovecz, Zoltán Kónya. Synergetic of Pt nanoparticles and H-ZSM-5 zeolites for efficient CO_2 activation: Role of interfacial sites in high activity, *Front. Mat.* (2019) doi: 10.3389/fmats.2019.00127

30. Yomaira J. Pagán-Torres, Tianfu Wang, Jean Marcel R. Gallo, Brent H. Shanks, and James A. Dumesic. Production of 5-Hydroxymethylfurfural from Glucose Using a Combination of Lewis and Brønsted Acid Catalysts in Water in a Biphasic Reactor with an Alkylphenol Solvent. *ACS Catal.*, 2012, *2* (6), pp 930–934.

31. Yuan Zhao, Shurong Wang, Haizhou Lin, Jingping Chen and Hao Xu[a]. Influence of a Lewis acid and a Brønsted acid on the conversion of microcrystalline cellulose into 5-hydroxymethylfurfural in a single-phase reaction system of water and 1,2-dimethoxyethane. RSC Advances. Issue 13, 2018, 7235-7242.